Characterization of the Degradation of HEPA Filters Protected by Different Spark Arrestors for Various Cutting Means and Cutting Conditions

Soleiman Bourrous, Mathieu Barrault, Laurent Ricciardi

Characterization of the degradation of HEPA filters protected by different spark arrestors for various cutting means and cutting conditions

Bourrous Soleiman[1]
Institut de Radioprotection et de Sûreté Nucléaire (IRSN), PSN-RES, SCA, Gif-Sur-Yvette, 91192, France
soleiman.bourrous@irsn.fr

Barrault Mathieu
Institut de Radioprotection et de Sûreté Nucléaire (IRSN), PSN-RES, SCA, Gif-Sur-Yvette, 91192, France
mathieu.barrault@irsn.fr

Ricciardi Laurent
Institut de Radioprotection et de Sûreté Nucléaire (IRSN), PSN-RES, SCA, Gif-Sur-Yvette, 91192, France
laurent.ricciardi@irsn.fr

ABSTRACT

The ageing of the nuclear installations induces new challenges regarding the containment of radioactive matter especially airborne contamination. The purification of the air using fibrous filters is the most widely used technology for the containment of this contamination. However, to ensure their role, they need to be protected. The release of incandescent particles cutting processes could reduce their efficiency. Many spark arrestors are available to protect the filters from hot particles. They are designed to be implemented upstream the filter. Three technologies of spark arrestors have been tested when they are exposed to a grinder or a plasma cutting process. The experiments have been performed for two different filters (450 and 1500 m^3/h flowrate). The particle size distribution of the aerosol produced by a plasma torch cutting has been measured and shows two characteristic modes for this kind of generation process. The filtration efficiency of the HEPA (High Efficiency Particulate Air) filter has been measured before and after the cutting (NF-EN-ISO-16170). During the experiments, the pressure drop of the HEPA filters has been measured to estimate their clogging rate. Results show that the plasma cutting is a more penalizing cutting process compared to metal grinder and that the metallic fibrous medium with the finest mesh has the better performances to protect filters from sparks. The cut length and the distance between the filter and the spark arrestor have also been studied, showing a limited impact on the degradation of the filtration efficiency.

[1]Corresponding author

INTRODUCTION

The safety of workers and environment during nuclear installation dismantling operations is a current issue for the different actors of this industry [2, 9]. The ability of companies to ensure dismantling without any radiological consequences needs to be demonstrated and therefore many works are dealing with this aspect [3, 5, 8-12]. The containment of airborne contamination released by the cutting of contaminated materials is mainly ensured by HEPA filters which are made of glass fibres [2]. This technology has many advantages in various operating conditions but, in a dismantling context, the presence of incandescent particles which may reach the filter can cause degradation of the fibers and, in consequence, lead to a decrease of the filtration efficiency and a possible fire development in the ventilation networks. Moreover, thermal cutting processes release ultrafine particles, leading to a very quick pressure drop increase. Many manufacturers propose spark arrestors to protect the filter from being affected by incandescent particles. Different technologies, based on inertial interception, are available on the market. It has been shown [9] that those devices are in some case inefficient to avoid filter degradation. Based on an experimental setup representative of the on-site operating conditions, this study aims to characterize the particle properties and the ability of three different spark arrestors to protect two different kinds of filters from being affected by particles produced by grinder or plasma cutting. This protection is evaluated by measuring the decontamination factor (DF) of the filters before and after each cutting operation. The decontamination factor is defined by the NF EN ISO 16170 as the ratio of the concentration of an aerosol, with a particle size distribution centred on 0.15 µm, upstream and downstream the filter.

MATERIAL AND METHODS

Test bench

To study the impact of the particles produced by dismantling activities on the containment of the radioactive pollution and the impact of the different commercial types of arrestors, a specific test bench has been developed [8,9]. This bench aims to reproduce realistic cutting conditions and to measure the properties of particles in terms of size, structure and temperature. Special attention is also paid on the evaluation of the efficiency of spark arrestor commercially available. The bench is composed of a cutting mean where cutting parameters (cutting speed, cutting length and trajectory…) are controlled (Figure 1). The distance between the spark arrestor and the filter can be changed and the flowrate of the filter is controlled.

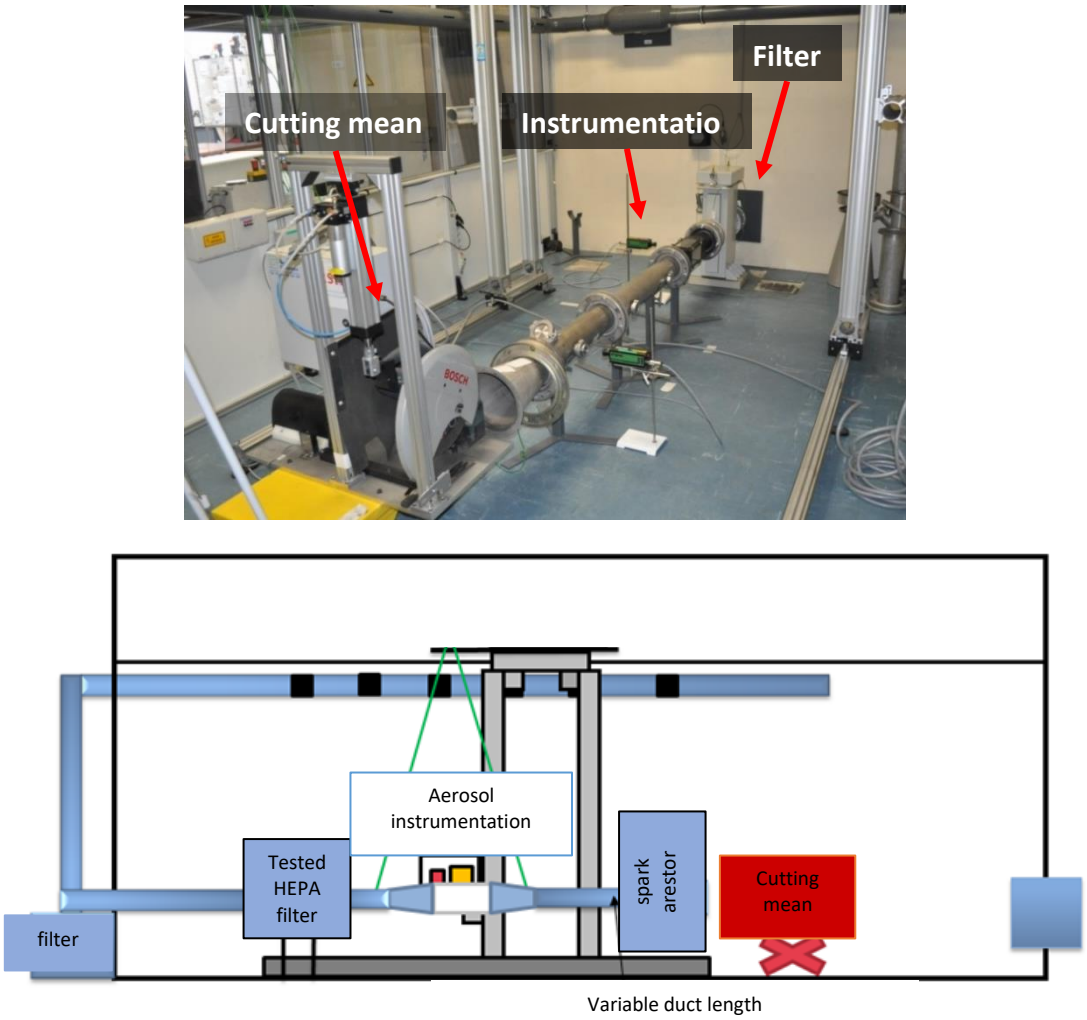

Figure 1: photo and schematic view of the test bench used in this study

Aerosol measurement of the fine fraction of the produced aerosol (5 to 1000 nm) is performed using a Grimm© 5.04.1 SMPS (Scanning Mobility Particle Sizer) l. A TSI© APS 3321 (Aerodynamic Particle Sizer) and an Andersen low pressure impactor sampling are also used for the larger fraction (0.3 to 10 µm).

Filters

Two different filters have been used in this study. Both of them are HEPA H14 (according to NF EN 1822 [13]) mini pleated filters and are provided by Camfil©. The filtration is ensured by a glass fiber medium. Those filters are classically used in the nuclear industry. Two models were used (respectively under the references DD and DC (respectively model 1501.37.00 and 1565.08.10) in the present paper, reference number is listed in result tables): a 450 m^3/h (double dihedral) one and a 1500 m^3/h (half-cell) one, for a nominal pressure drop of 250 Pa. Filters have been certified according to the CTHEN specification (CTHEN is the French Technical Centre for Nuclear Equipment Certification, belonging to IRSN [14]). A picture of the upstream side of the filters is presented in Figure 2. The exposed surface of those filters is different and may influence their resistance to spark aggressions.

The Decontamination Factor was measured according to the Annex C of the NF EN ISO 16170 [15], by using a soda-fluorescein aerosol with a mass median diameter of 0.15 µm.

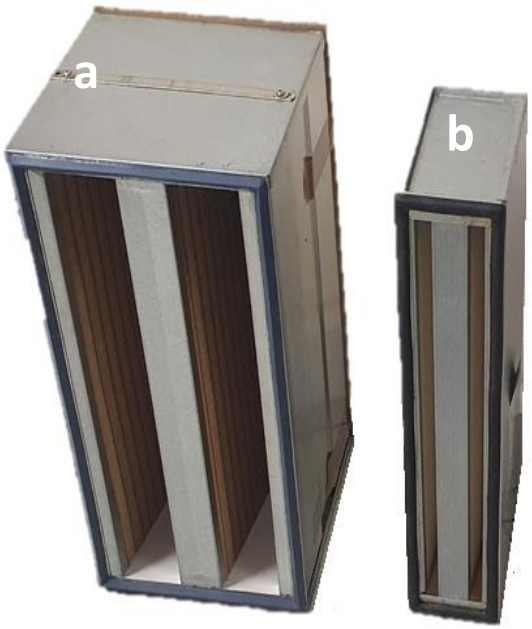

Figure 2: upstream picture of the filters used in this study (a) 210 mm / 130 mm/ 600 mm for a nominal flowrate of 450 m^3/h (b) 210 mm / 305 mm/ 600 mm for a nominal flowrate of 1500 m^3/h

Spark arrestors

Three different models of spark arrestors have been tested (Figure 3). Those models are currently used in the dismantling operations. The first one is a wire mesh overlay with meshes of different sizes (the finest mesh is around 100 µm) and is provided by Camfil© (Model 62719900, under the reference TM in the present paper (for *"Treillis Metallique",* Metallic mesh). The second one, also provided by Camfil©, is made of a coarser metallic fibrous medium protected by steel plates (Model 14656008, under the reference TM21 (For "*treillis Metallique 2 en 1"*, two in one metallic wire mesh) in the present paper). The third one is provided by Vectori© and is made of steel plates organised in chicane without fibrous media (Model FCSI4844, under the reference CH (For "*Chicane*", simple steel plates) in the present paper).

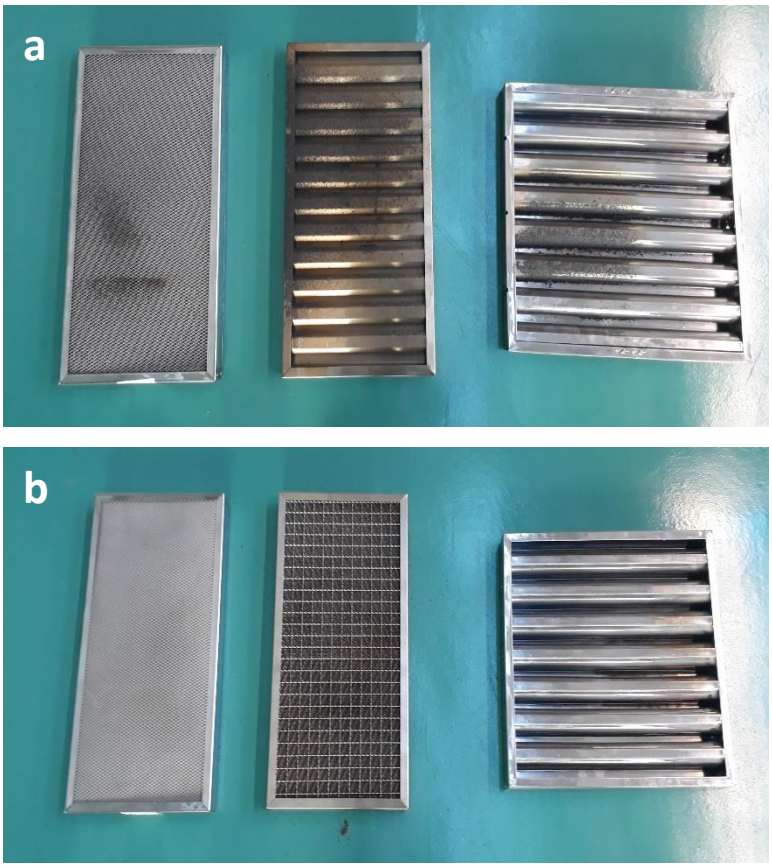

Figure 3: upstream (a) and downstream (b) view of the spark arrestors tested (from left to right, 600 mm x 300 mm metallic wire mesh (TM), 600 mm x 300 mm, two in one metallic wire mesh (TM21) and 490 mm x 490 mm simple steel plates (CH)

Cutting tools

A grinder and a plasma torch have been used. The cut material is stainless steel which is often met in nuclear industry (316L) with a thickness of 4 mm. Due to the differences of those two processes, different cutting configurations have been used and are presented in Figure 4.

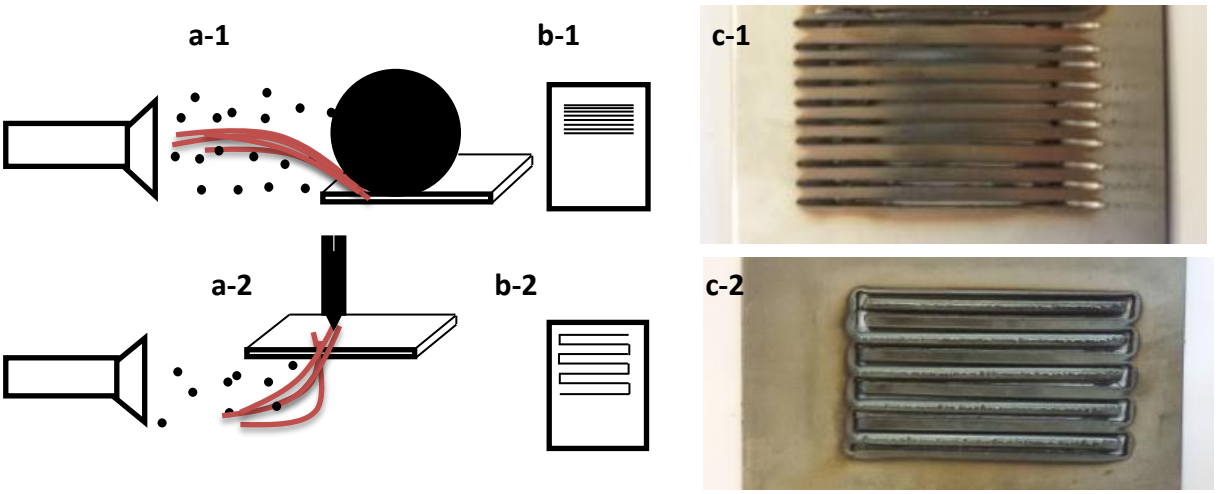

Figure 4: position of the cutting from the entrance of the test bench (a), schema (b) and pictures (c) of the cutting for a metal grinder (c-1) and a plasma torch (c-2)

The disk of the grinder has a diameter of 350 mm, a thickness of 3 mm and a rotational speed of 3200 RPM the force applied on the device is 78 N. Plasma torch is referenced TP in this paper and grinder is referenced Di. Two cutting lengths have been tested corresponding to 10 or 40 cuts of 140 mm.

Test matrix

The influent variables considered in this study are:

- the cutting tool which has an influence on the particle size distribution;
- the cut length (number of cuts) which influences the mass of particles accumulated, leading to a higher clogging but also which increases the probability of degradation;
- the duct length (distance between the spark arrestor and the filter) which should reduce the amount of degrading particles (due to inertial deposition and sedimentation phenomena).

In this study, many different configurations have been tested.

RESULTS

Particle size distribution upstream the spark arrestor for a cutting done with a plasma torch

Due to the very high concentration of particles, two Palas© VKL 10 diluters were used (this also avoids the thickest particles to be collected). As expected [7] for thermal cutting processes, two populations of particles can be distinguished. Figure 5b presents the particle size distribution of thick particles (over 0.5 µm) measured by a TSI© aerodynamic particle sizer. Most of the particles in this size range are spherical particles produced from melted material [10]. They may induce a degradation of the collection efficiency of the filter due to their high temperature. Figure 5a presents the fine fraction of this aerosol (measured with a TSI Scanning Mobility Particle Sizer SMPS) mainly composed by aggregates formed by condensation processes of vaporized material. This aerosol fraction, not identified with grinder cutting ([9]), is responsible for the very quick pressure drop increase of the filters.

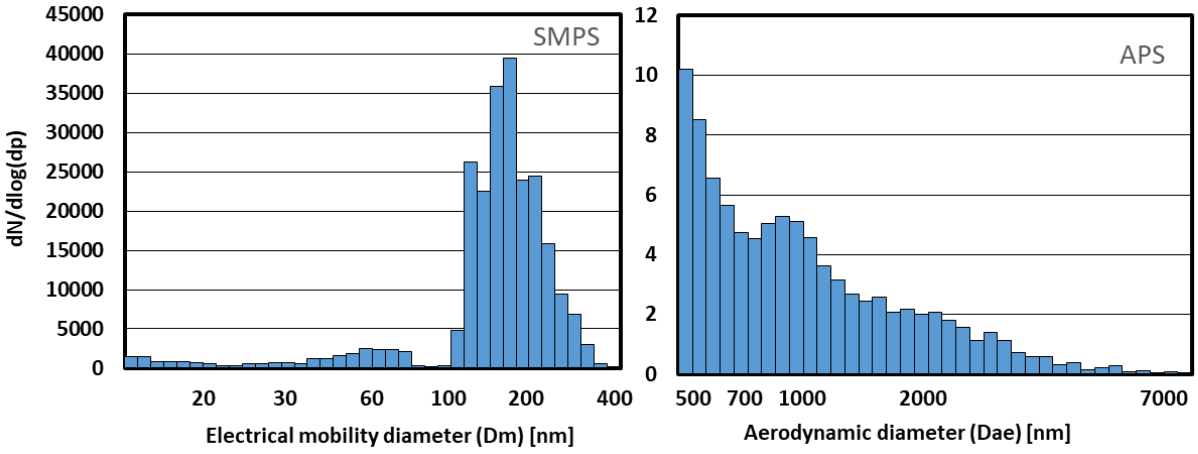

Figure 5: particle size distribution measured upstream the filter for a plasma torch cutting ((a) SMPS, (b) APS)

Particle size distribution downstream the spark arrestor for a cutting done with a plasma torch

The concentration of particles under 15 µm has been considered in this study by the use of the Andersen impactor. However, in real operating conditions, due to their inertia, most of them are deposited in the duct upstream the filter. Figure 6 presents the particle size distribution obtained downstream the different spark arrestors. In agreement with the measurements performed upstream the spark arrestors (Figure 5), the particle size distribution is bimodal and we can observe that the collection efficiency of the metallic wire mesh ™ model is the most important for micron particles. On the contrary, the efficiency is lower for the simple steel plates (CH) model.

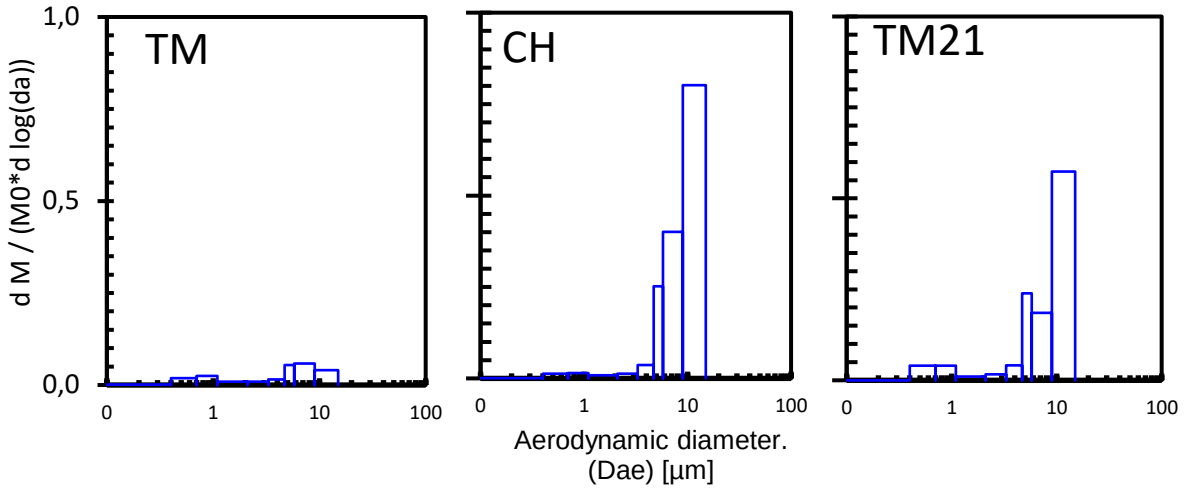

Figure 6: particle size distribution of the particles measured downstream the different spark arrestors

Impact of the aerosol on the filter clogging

Some experiments using a grinder plate and a plasma torch have been performed without spark arrestors in order to compare the impact of the different aerosols on the pressure drop (and thereby the lifetime) of filters. Flowrate and pressure drop have been monitored during the cutting for a similar cut length (corresponding to a length of 140 cm). Figure 7 shows the results as a function of time for half the nominal filtration flowrate and for a double dihedral filter.

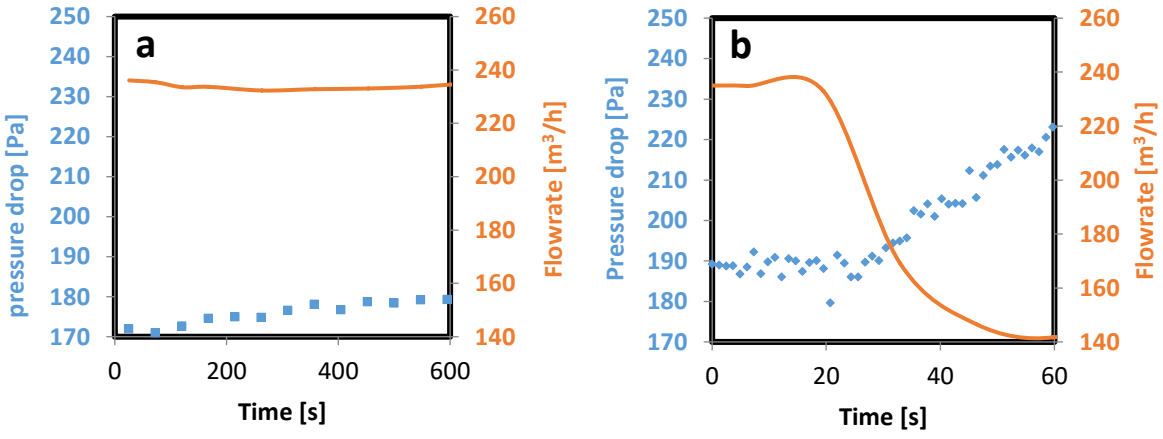

Figure 7: evolution of flowrate and pressure drop of double dihedral filter during grinder plate (a) and plasma torch (b) cutting

One can notice that plasma cutting induced a very quick pressure drop increase leading to a significant decrease of the flowrate passing through the filter (Figure 7-b). Beyond the issue of the filtration efficiency, those results show the necessity to take into account the impact of the kind of cutting tool used and the impact of the containment efficiency regarding the flowrate of the filter. This point is very important because most of the time, in dismantling sites, only the filter pressure drop is monitored, which is insufficient to prevent a drastic decrease of the extraction flowrate. This trend confirms the impact of submicron particle fraction released by this cutting mean on fibrous filters, and spark arrestors are not supposed to avoid this phenomenon.

Impact of the filter type used on the filtration efficiency

The design of the filters, in terms of flowrate but also in terms of exposition of the filter media to potential degradations, may influence the resistance of the filter to incandescent particles. Table 1 summarizes the results obtained in the different conditions for both filters tested at half and at the nominal flowrate.
One can notice, for 5 tests, an increase of the decontamination factor DF (see values in green). This is due to the accumulation of particles in the filter. There is then a competition between the filtration efficiency increasing due to particle accumulation and the degradation of the medium which induces leaks and therefore reduces the filtration efficiency (see values in red). The evaluation of the vulnerability needs therefore to take into account both increase and decrease of the DF. Due to the more open angle of the filter dihedral and to the higher flowrate, the half-cell filter is much more vulnerable to the degradation than the double dihedral filter, especially when the distance between the spark arrestor and the filter is short (distance 2).

Table 1 : experiments performed in the same conditions with two different filters

	Filter design																	
	DD (double dihedral, 450 m^3/h)									DC (half-cell, 1500 m^3/h)								
Tool	Number of cuts	Spark arrestor	Filter	Distance	Filtration velocity	DF before cutting	DF after cutting	Relative difference		Tool	Number of cuts	Spark arrestor	Filter	Distance	Filtration velocity	DF before cutting	DF after cutting	Relative difference
Di	10	TM21	DD	1	Vn	25 600	16 800	-34%(↓)		Di	10	TM21	DC	1	Vn	62 053	45 630	-26% (↑)
Di	10	TM21	DD	2	Vn	25 966	98 132	278%(↑)		Di	10	TM21	DC	2	Vn	44 327	57 255	29% (↓)
Di	40	TM21	DD	1	Vn	169 000	49 800	-71%(↓)		Di	40	TM21	DC	1	Vn	64 974	161 626	149% (↑)
Di	40	TM21	DD	2	Vn	25 795	50 000	94%(↑)		Di	40	TM21	DC	2	Vn	52 007	6 740	-87% (↓)
TP	10	CH	DD	2	Vn	10 916	949	-99%(↓)		TP	10	CH	DC	2	Vn	73 408	866	-99% (↓)
TP	10	TM21	DD	2	Vn/2	112 395	91 514	-19%(↓)		TP	10	TM21	DC	2	Vn/2	221 947	5 352	-98% (↓)
TP	10	TM21	DD	2	Vn	28 626	71 878	151%(↑)		TP	10	TM21	DC	2	Vn	42 431	4 542	-89% (↓)
Number of tests with DF ↑								3		Number of tests with DF ↑								2
Number of tests with DF↓								4		Number of tests with DF↓								5
Mean relative difference								43%		Mean relative difference								-32%

Impact of the type of cutting tool used

The experiments performed in the same conditions with the cutting tool as only difference are listed in Table 2. One could notice that the mean DF evolution, for those various experiments, is positive. This could tend to conclude to a higher contribution of the clogging of the filters than on its degradation. However, some differences can be observed between the results obtained with the grinder and those obtained with the plasma torch. First, the mean increase of the DF is 50% for the tests performed with the grinder, against only 14% for the plasma torch. In addition, only 25% of the filters tested with a grinder have a decrease in the DF value, against 58 % for filters exposed to a plasma torch aerosol. Finally, for 9 of the 12 tests, the value of the relative difference quantifying the DF evolution decreases when using a plasma torch, in comparison with the grinder use. Hence, all these observations show a greater impact of the plasma torch cutting on the filtration efficiency. Nevertheless, it should be noted that only one of the filters tested with the plasma torch has a DF lower than 5 000 (DF = 866), which is the minimum value required by the CTHEN specification for the efficiency of a HEPA filter.

Table 2: experiments performed in the same conditions with two different cutting tools

	Cutting tool																
	Di (grinder)									TP (plasma torch)							
Tool	Number of cuts	Spark arrestor	Filter	Distance	Filtration velocity	DF before cutting	DF after cutting	Relative difference		Tool	Number of cuts	Spark arrestor	Filter	Distance	Filtration velocity	DF before cutting	DF after cutting	Relative difference
Di	10	CH	DC	1	Vn	41 263	29 297	-29%(↓)		TP	10	CH	DC	1	Vn	118 781	21 899	-82% (↓)
Di	10	CH	DC	1	Vn/2	135 621	141 329	4%(↑)		TP	10	CH	DC	1	Vn/2	331 164	14 042	-96% (↓)
Di	10	CH	DC	2	Vn	34 064	27 290	-20%(↓)		TP	10	CH	DC	2	Vn	73 408	866	-99% (↓)
Di	10	TM21	DC	2	Vn	44 327	57 255	29%(↑)		TP	10	TM21	DC	2	Vn	42 431	4 542	-89% (↓)
Di	10	TM21	DD	2	Vn	25 966	98 132	278%(↑)		TP	10	TM21	DD	2	Vn	28 626	71 878	151% (↑)
Di	10	TM	DC	1	Vn	38 364	48 439	26%(↑)		TP	10	TM	DC	1	Vn	61 787	255 866	314% (↑)
Di	10	TM	DC	1	Vn/2	101 872	147 271	45%(↑)		TP	10	TM	DC	1	Vn/2	324 934	359 091	11% (↑)
Di	10	TM	DC	2	Vn	52 637	97 188	85%(↑)		TP	10	TM	DC	2	Vn	43 944	42 431	-3% (-)
Di	10	TM	DC	2	Vn/2	127 068	195 810	54%(↑)		TP	10	TM	DC	2	Vn/2	106 478	34 213	-68% (↓)
Di	40	TM21	DD	2	Vn	25 795	50 000	94%(↑)		TP	40	TM21	DD	2	Vn	54 841	21 726	-60% (↓)
Di	40	TM	DC	1	Vn	97 979	91 643	-6%(-)		TP	40	TM	DC	1	Vn	69 262	166 122	140% (↑)
Di	40	TM	DC	1	Vn/2	115 303	164 297	42%(↑)		TP	40	TM	DC	1	Vn/2	214 881	314 064	46% (↑)
Number of tests with DF ↑								9		Number of tests with DF ↑								5
Number of tests with DF↓								3		Number of tests with DF↓								7
Mean relative difference								50%		Mean relative difference								14%

Impact of the type of spark arrestor used

Table 3 presents the different tests performed in the same conditions with different spark arrestors. Results show a significant trend. The simple steel plates (CH) are clearly inefficient: in all conditions, the efficiency of the filter decreases after the cutting phases. In addition, for two of the tests performed, DF decreases far below the required value of 5 000 for a HEPA filter certified by the CTHEN (DF = 949 and 866). On the contrary, Table 3 shows that the most efficient technology is the simple metallic wire mesh (TM) comprising a fibrous medium with a fine mesh (≈ 100 µm).

Table 3: experiments performed in the same conditions with three different spark arrestors

		Model of spark arrestor															
		TM (wire mesh overlay)								TM21 (fibrous medium + steel plates)							
Tool	Number of cuts	Spark arrestor	Filter	Distance	Filtration velocity	DF before cutting	DF after cutting	Relative difference		Tool	Number of cuts	Spark arrestor	Filter	Distance	Filtration velocity	DF before cutting	DF after cutting	Relative difference
Di	10	TM	DC	1	Vn	38 364	48 439	26%(↑)		Di	10	TM21	DC	1	Vn	62 053	45 630	-26% (↓)
Di	10	TM	DC	2	Vn	52 637	97 188	85%(↑)		Di	10	TM21	DC	2	Vn	44 327	57 255	29% (↑)
Di	40	TM	DC	1	Vn	97 979	91 643	-6%(-)		Di	40	TM21	DC	1	Vn	64 974	161 626	149% (↑)
Di	40	TM	DC	2	Vn	25 192	45 234	80%(↑)		Di	40	TM21	DC	2	Vn	52 007	6 740	-87% (↓)
TP	10	TM	DC	2	Vn	43 944	42 431	-3%(-)		TP	10	TM21	DC	2	Vn	42 431	4 542	-89% (↓)
TP	10	TM	DC	2	Vn/2	106 478	34 213	-68%(↓)		TP	10	TM21	DC	2	Vn/2	221 947	5 352	-98% (↓)
Number of tests with DF ↑								3		Number of tests with DF ↑								2
Number of tests with DF↓								3		Number of tests with DF↓								4
Mean relative difference								19%		Mean relative difference								-20%

	CH (chicane with steel plates)								
	Tool	Number of cuts	Spark arrestor	Filter	Distance	Filtration velocity	DF before cutting	DF after cutting	Relative difference
	Di	10	CH	DC	1	Vn	41 263	29 297	-29% (↓)
	Di	10	CH	DC	2	Vn	34 064	27 290	-20% (↓)
	Di	40	CH	DC	1	Vn	132 304	128 063	-3% (-)
	Di	40	CH	DC	2	Vn	84 781	7 642	-91% (↓)
	TP	10	CH	DC	2	Vn	73 408	866	-99% (↓)
	TP	10	CH	DC	2	Vn/2	884 597	547	-99% (↓)
	Number of tests with DF ↑								0
	Number of tests with DF↓								6
	Mean relative difference								-57%

Impact of the distance between the filter and the spark arrestor

Since the thickest particles have an impact on the degradation of the medium, it is to expect that a longer distance between the spark arrestor and the filter should reduce significantly its degradation. This is mainly for two reasons:

- the temperature of the sparks should decrease as their transportation time increases,
- thicker particles should settle as the length increases.

The results obtained (Table 4) do not seem to confirm those assumptions. For the two distances considered, half of the values decreases and the other half increases. On average, one can observe a slight increase of the DF, which is of the same order for both cases (17% for a 30 cm distance and 19% for 270 cm). Nevertheless, some differences seems to be observable according to the type of cutting tool used: when the distance between the spark arrestor and the filter is shorter, the relative difference quantifying the DF evolution decreases for the plasma torch cutting, whereas for the grinder cutting, this relative difference generally increases (except for three tests). This conclusion needs to be nuanced by the dispersion of the DF obtained for the different experiments.

Table 4 : experiments realized in the same condition with two different cutting distance

Distance between the filter and the spark arrestor																		
30 cm									270 cm									
Tool	Cut length	Spark arrestor	Fitlers design	Duct length	Filtration flowrate	DF new	DF after cutting	Difference	Tool	cut length	spark arrestor	Fitlers design	Duct length	Filtration flowrate	DF new	DF after cutting	Difference
Di	10	CH	DC	1	VN	41 263	29 297	-29%(↓)	Di	10	CH	DC	2	VN	34 064	27 290	-19,89%(↓)
Di	10	CH	DC	1	VN/2	135 621	141 329	4,21%(-)	Di	10	CH	DC	2	VN/2	111 475	150 698	35,19%(↑)
Di	10	TM21	DC	1	Vn	62 053	45 630	-26,5%(↓)	Di	10	TM21	DC	2	Vn	44 327	57 255	29,2%(↑)
Di	10	TM21	DD	1	Vn	25600	16800	-34,38%(↓)	Di	10	TM21	DD	2	Vn	25966	98132	277,92%(↑)
Di	10	TM	DC	1	VN	38 364	48 439	26,26%(↑)	Di	10	TM	DC	2	VN	52 637	97 188	84,64%(↑)
Di	10	TM	DC	1	VN/2	101 872	147 271	44,57%(↑)	Di	10	TM	DC	2	VN/2	127 068	195 810	54,1%(↑)
Di	40	CH	DC	1	VN	132 304	128 063	-3,21%(-)	Di	40	CH	DC	2	VN	84 781	7 642	-90,99%(↓)
Di	40	CH	DC	1	VN/2	163 469	249 949	52,9%(↑)	Di	40	CH	DC	2	VN/2	318 362	125 720	-60,51%(↓)
Di	40	TM21	DC	1	Vn	64 974	161 626	148,8%(↑)	Di	40	TM21	DC	2	Vn	52 007	6 740	-87%(↓)
Di	40	TM21	DD	1	Vn	169000	49800	-70,53%(↓)	Di	40	TM21	DD	2	Vn	25795	50000	93,84%(↑)
Di	40	TM	DC	1	VN	97 979	91 643	-6,47%(-)	Di	40	TM	DC	2	VN	25 192	45 234	79,56%(↑)
Di	40	TM	DC	1	VN/2	115 303	164 297	42,49%(↑)	Di	40	TM	DC	2	VN/2	25 452	60 287	136,87%(↑)
Tp	10	CH	DC	1	Vn	118 781	21899	-81,56%(↓)	Tp	10	CH	DC	2	Vn	73 408	866	-98,82%(↓)
Tp	10	TM	DC	1	Vn	61 787	255 866	314,11%(↑)	Tp	10	TM	DC	2	Vn	43 944	42 431	-3,44%(-)
Tp	10	TM	DC	1	Vn/2	324 934	359 091	10,51%(↑)	Tp	10	TM	DC	2	Vn/2	106 478	34 213	-67,87%(↓)
↑								8	↑								8
↓								7	↓								7
Mean								26,15%	Mean								24,19%

Impact of the cut length

The cut length is proportionally related to the amount of particle produced and, therefore, this variable induces a higher clogging of the filter (increasing its efficiency) and a higher probability for thick incandescent particles to reach the filter and to deteriorate it. In parallel, if the airflow resistance of the medium increases due to its clogging, the impact of leaks on the filtration efficiency will also increase.

The experiments performed and summarized in Table 5 show that the degradation of filters is, on average, more important when the number of cuts is higher. Indeed, if a mean DF increase is observed over the 16 experiments performed, this increase is 57 % when 10 cuts are performed, against 23 % for 40 cuts. In addition, we can notice a decrease of the filter efficiency for 5 tests when 10 cuts are performed, against 7 tests with 40 cuts. Lastly, one can observe that, in most cases, the relative difference related to the evolution of the DF value decreases when the number of cuts increases from 10 to 40 cuts.

However, an evaluation of the clogging dynamics and degradation rate of the medium should be conducted to conclude on this impact. One could notice that those conclusions are similar for all tested configurations.

Table 5 : experiments realized in the same condition with two different cutting length

Number of cuts (14 cm each)																	
10 cuts									40 cuts								
Tool	cut length	spark arrestor	Fitlers design	Duct length	filtration flowrate	DF new	DF after cutting	Difference	Tool	cut length	spark arrestor	Fitlers design	Duct length	filtration flowrate	DF new	DF after cutting	Difference
Di	10	CH	DC	1	VN	41 263	29 297	-29%(↓)	Di	40	CH	DC	1	VN	132 304	128 063	-3,21%(↓)
Di	10	CH	DC	1	VN/2	135 621	141 329	4,21%(-)	Di	40	CH	DC	1	VN/2	163 469	249 949	52,9%(↑)
Di	10	CH	DC	2	VN	34 064	27 290	-19,89%(↓)	Di	40	CH	DC	2	VN	84 781	7 642	-90,99%(↓)
Di	10	CH	DC	2	VN/2	111 475	150 698	35,19%(↑)	Di	40	CH	DC	2	VN/2	318 362	125 720	-60,51%(↓)
Di	10	TM21	DC	1	Vn	62 053	45 630	-26,5%(↓)	Di	40	TM21	DC	1	Vn	64 974	161 626	148,8%(↑)
Di	10	TM21	DC	2	Vn	44 327	57 255	29,2%(↑)	Di	40	TM21	DC	2	Vn	52 007	6 740	-87%(↓)
Di	10	TM21	DD	1	Vn	25600	16800	-34,38%(↓)	Di	40	TM21	DD	1	Vn	169000	49800	-70,53%
Di	10	TM21	DD	2	Vn	25966	98132	277,92%(↑)	Di	40	TM21	DD	2	Vn	25795	50000	93,84%(↑)
Di	10	TM	DC	1	VN	38 364	48 439	26,26%(↑)	Di	40	TM	DC	1	VN	97 979	91 643	-6,47%(↓)
Di	10	TM	DC	1	VN/2	101 872	147 271	44,57%(↑)	Di	40	TM	DC	1	VN/2	115 303	164 297	42,49%(↑)
Di	10	TM	DC	2	VN	52 637	97 188	84,64%(↑)	Di	40	TM	DC	2	VN	25 192	45 234	79,56%(↑)
Di	10	TM	DC	2	VN/2	127 068	195 810	54,1%(↑)	Di	40	TM	DC	2	VN/2	25 452	60 287	136,87%(↑)
Tp	10	TM21	DD	2	Vn/2	112 395	91 514	-18,58%(↓)	Tp	40	TM21	DD	2	Vn	54 841	21 726	-60,38%(↓)
Tp	10	TM21	DD	2	Vn	28 626	71 878	151,09%(↑)	Tp	40	TM21	DD	2	Vn/2	149 981	157 764	5,19%(↑)
Tp	10	TM	DC	1	Vn	61 787	255 866	314,11%(↑)	Tp	40	TM	DC	1	Vn	69 262	166 122	139,85%(↑)
Tp	10	TM	DC	1	Vn/2	324 934	359 091	10,51%(↑)	Tp	40	TM	DC	1	Vn/2	214 881	314 064	46,16%(↑)
↑				11					↑				9				
↓				5					↓				7				
Mean				56,47%					Mean				22,91%				

CONCLUSION

The different configurations tested in this study show that the degradation of HEPA filters by sparks produced by different cutting processes requires to be considered even with the use of commercial spark arrestors devices. The different tests performed show that:

- the opening of the double dihedral filters, beyond the impact of the flowrate, has an impact on their resistance when exposed to sparks from cutting processes;
- as expected, plasma cutting has a strong impact on the pressure drop of the filters. Moreover, the decrease of the DF is more important when using this kind of tool compared to grinding plate. This conclusion could reasonably be extrapolated to other thermal cutting processes producing thin particles [2], [3], [4], [7];
- between the three technologies tested in this work, simple metallic fibrous media with a thin mesh shows a better protection of the filter. This is true for DF but also for the clogging of the filter. By acting like a pre-filtration stage [16], the lifetime of the filter is also improved;
- the clogging of the filter has an influence on the filters efficiency which needs to be further investigated. Indeed, the loaded filter has an increasing efficiency but its increase in terms of pressure drop also induces a preferential path of the air through the leak. In this study, for the two cut lengths considered, it has been shown that the filtration performances decreases, both in terms of pressure drop and filtration efficiency;
- two configurations of duct length between the filter and the spark arrestor have been tested (30 cm and 270 cm).A differences has been noticed in terms of performances evolutions. The oxidation of iron particles in the air [17] can explain such a measurement. The dispersion of the experimental values obtained requires further phenomenological investigations to ensure the reliability of this assumption.

To summarize, all experiments performed in this study give operational trends to design the air purification strategy in dismantling sites using HEPA filters protected by commercial devices. Some phenomenological studies need to be done to understand and/or model all phenomena occurring in this situation.

ACKNOWLEDGEMENT

The authors would like to thank EDF, in particular Luc Lafanechère, for funding this research program and for helping considering on the current practices in dismantling sites.

NOMENCLATURE

CH	Steel plates spark arrestor
DC	Half cell
DD	double dihedral
DF↑	Decontamination factor increase after cutting
DF↓	Decontamination factor decrease after cutting
DF_{after}	Decontamination factor after cutting
DF_{before}	Decontamination factor before cutting
Di	Grinder
TM	Metallic mesh spark arrestor
TM21	2 in one metallic mesh spark arrestor
Tp	Plasma torch

REFERENCES

[1] Artous, S., Norvez, O., Teppe, A.L., 2011. "Etude de l'impact d'étincelles produites par une disqueuse sur l'efficacité de filtres THE". Technical report IRSN/DSU/SERAC/LECEV/11-32.

[2] CETIER, P., 1989. "Caractérisation des transferts de contaminants lors des découpes thermiques et mécaniques d'échantillons métalliques". Ph. D. thesis, CNAM.

[3] Bach, F.W., Steiner, H., Schreck, G., Pilot, G., 1993. "Analysis of results obtained with different cutting techniques and associated filtration systems for the dismantling of radioactive metallic components". Technical report, Commission of the European Communities. EUR 14213.

[4] Bishop, A., 1989. "Ventilation and filtration techniques for handling aerosols produced by thermal cutting operations". Technical Report, Commission of the European Communities. EUR 12321.

[5] Laborde, J.C., 1996. "Performances de dispositifs de protection des filtres THE contre les aérosols incandescents". Technical Report IRSN/DSU/SERAC/LECEV/96-21.

[6] Marchal, P., Porcheron, E., 2014, September-October. R&D : "Impact des particules incandescentes dans les réseaux de ventilation". Revue Générale Nucléaire (5), 55-59. https://doi.org/10.1051/rgn/20145055

[7] Cetegen, B.M., Yu, W., 1999. "In-situ particle temperature, velocity and size measurements in DC Arc Plasma thermal sprays". Journal of Thermal Spray Technology, 8(1), pp. 57-67. https://doi.org/10.1361/105996399770350575

[8] Marchal, P., Porcheron, E., Grehan, G., Lafanechere, L., Walter, J., Gelain, T., 2015. "Characterization of incandescent particles emitted by a cut-off grinder during decommissioning operations for evaluating filter degradation". J Nucl Eng Radiat Sci., https://doi.org/10.1115/1.4029343

[9] Marchal, P., Porcheron, E., Lafanechere, L., Walter, J., Grehan, G., 2013. "Incandescent particle characterisation emitted by a cut-off wheel grinder during decommissioning operations for evaluating filters degradation". International Conference on Nuclear Engineering (ICONE21). Chengdu, China. https://doi.org/10.1115/ICONE21-15353

[10] Newton, G.J., Hoover, M.D., Barr, E.D., Wong, B.A., Ritter, P.D., 1987. "Collection and characterization of aerosols from metal cutting techniques typically used in decommissioning nuclear facilities". American Industrial Hygiene Association journal, 48(11), pp. 922-932. https://doi.org/10.1115/ICONE21-15353

[11] Pilot, G., Fauvel, S., Gosse, X., Dinechin, G., Vernhet, D., 2006. "Dismantling of Evaporators by Laser Cutting: Measurement of Secondary Emissions". In : 14th International Conference on Nuclear Engineering. ASME Digital Collection, pp. 519-525. https://doi.org/10.1115/ICONE14-89709

[12] Hoover, M.D., Newton, G.J., Barr, E.D., Wong, B.A., 1982. "Aerosols from metal cutting techniques typical of decommissioning nuclear facilities - Inhalation hazards and worker protection". Seattle, WA: International Decommissioning Symposium. - http://inis.iaea.org/search/search.aspx?orig_q=RN:15002072

[13] NF EN 1822-1 April 2019 "Filtre à air à très haute efficacité (EPA, HEPA et ULPA) – Partie 1 : classification essais de performance et marquage"

[14] Specification for filters used for nuclear applications, Institut de Radioprotection et de Sûreté Nucléaire, IRSN/CTHEN n° 93-030, 2020

[15] ISO 16170 :2016 "Méthode d'essai in situ pour les systèmes filtrants à très haute efficacité dans les installations industrielles"

[16] Charvet, A., Pacault, S., Bourrous, S., Thomas D., 2018 "Association of fibrous filters for aerosol filtration in predominant Brownian diffusion conditions". Separation and Purification Technology, 2018, vol. 207, pp. 420-426. https://doi.org/10.1016/j.seppur.2018.06.045

[17] Paidassi, J., 1958. "The kinetics of the air oxidation of iron in the range 700-1250°C". Acta Metallurgica, 6(3), pp. 184-194.

Figure Captions List

Fig. 1 photo and schematic view of the test bench used in this study

Fig. 2 upstream picture of the filters used in this study (a) 210 mm / 130 mm/ 600 mm for a nominal flowrate of 450 m^3/h (b) 210 mm / 305 mm/ 600 mm for a nominal flowrate of 1500 m^3/h

Fig. 3 upstream (a) and downstream (b) view of the spark arrestors tested (from left to right, 600 mm x 300 mm metallic wire mesh (TM), 600 mm x 300 mm, two in one metallic wire mesh (TM21) and 490 mm x 490 mm simple steel plates (CH)